Journal of Power Sources, *38* (1992) 351–362

Multinary alloy electrodes for solid state batteries I. A phase diagram approach for the selection and storage properties determination of candidate electrode materials

A. Anani* and R. A. Huggins
Department of Materials Science and Engineering, Stanford University, Stanford, CA 94305 (USA)

(Received September 4, 1991; in revised form December 12, 1991)

Abstract

The desire to produce high specific energy rechargeable batteries has led to the investigation of ternary alloy systems for use as negative electrode components in lithium-based cells. The addition of a third component to a binary alloy electrode could result in a significant change in the thermodynamic and/or kinetic behavior of the electrode material, depending on the relevant phase diagram and the crystal structures of the phases present. The influence of ternary phase diagram characteristics upon the thermodynamic properties and specific energies of multi-component electrodes is discussed with lithium–silicon-based systems as an illustration. It is shown that the electrode potentials (and thus specific energies of the ensuing cell) as well as the theoretical lithium capacities of electrodes based on these ternary alloy modifications can be significantly increased with respect to their present day binary counterpart.

Introduction

Over the years, a vast amount of research work has been carried out on the development of alloy electrodes for use as anodes in lithium-based cells. The use of these alloys as electrodes imply reduced cell voltages, and thus specific energy, but at the same time may lead to significant improvement in the cycle life, performance and safety of the cells for which they are employed. Two alloys that are currently being used extensively, especially in intermediate temperature cells, are those based on the two-phase Li–Al [1, 2] and Li–Si [3, 4] systems. Operating thermodynamic properties of these alloy systems are +300 mV versus Li and 0.660 A h/g theoretical capacity for the $Li_yAl(0.08<y<0.9)$ system at 400 °C and +158 mV versus Li and 0.464 A h/g capacity for the $Li_ySi(2.33<y<3,2)$ system at 415 °C. Other anode materials that are currently being investigated include graphitic carbon and several other intercalation compounds.

In the search for alloys with better performance, one is not just restricted to binary systems alone. Ternary alloy systems may be considered as well, especially when

*Author to whom correspondence should be addressed. Present address: Center for Electrochemical Systems and Hydrogen Research, Texas A&M University, College Station, TX 77843, USA.

0378-7753/92/$5.00 © 1992 – Elsevier Sequoia. All rights reserved

they involve materials of lower weight with potentials that are close to that of pure lithium. The addition of a third component to a binary alloy electrode could result in a significant change in either the thermodynamic or kinetic behavior of the electrode material, depending on the relevant phase diagram and the crystal structures of the phases present.

In this work, the principles of ternary thermodynamics is applied to lithium alloys in evaluating the suitability and choice of prospective negative electrode materials. Materials based on the lithium–silicon system which exhibit behavior reminiscent of a reconstitution reaction whereby the electrode potential does not change during intercalation and deintercalation of the electroactive species and that can achieve high energy are considered. The principles and methodology that is described in this work may also be applicable to the screening process of candidate positive electrode materials.

General principles and methodology

Alloy electrode potentials and their corresponding compositional capacities are important thermodynamic parameters if an electrochemical cell is to be useful as an energy storage device. These parameters are easily derived from the thermodynamic free energies and the relevant phase diagrams of the respective candidate electrode materials systems. Thus to evaluate the suitability of ternary alloy materials as electrodes in electrochemical cells, it is pertinent to know the thermodynamic properties of the system in question. If one identifies the phases that are stable in any ternary system, and data on their respective Gibbs free energy of formation, or in fact, free energy at the operating temperature are available, one can construct the isothermal phase diagram representing the three component system. If these phases are assumed to have very narrow composition ranges, then they can be represented as point-phases on the phase diagram. The whole isothermal section will then be divided into triangles of three-phase equilibria, bounded by lines of two-phase equilibrium. The principles and procedures for the construction of multinary phase diagrams, and in particular, of a three-component system, have been discussed previously [5–10], and so will not be repeated here. However, such phase diagrams shall be used as a thinking tool to evaluate thermodynamic compatibilities between phases, and to interpret the reactions that take place, in a lithium-based system.

The understanding of the use of these phase diagrams as tools to interpret phase equilibrium reactions rests on the understanding of the basic types of electrode reactions themselves. These solid state electrode reactions can generally be divided into two groups: insertion reactions, in which the composition of the solid solution changes, and reconstitution reactions, in which the identity and amounts of the phases present can change.

For a general reaction of the type

$$B + xA \rightleftharpoons A_xB \tag{1}$$

where A is considered to be the electroactive species, the free energy change of the reaction, ΔG_{rxn}, is simply the sum of the products of free energies, G_i, or free energies of formation, $\Delta G_{f,i}$, and the stoichiometric coefficient, ν_i, of the products and reactants, where ν is negative for reactants and positive for products. That is,

$$\Delta G_{rxn} = \prod_i \nu_i G_i = \prod_i (\nu_i \, \Delta G_{f,i}) \tag{2}$$

The free energy change of the reaction is thus related to the activities of the various components and also to the electromotive force, E, of an appropriately designed electrochemical cell via the Nernst relationship:

$$\Delta G_{rxn} = -nFE = RT \ln K; \qquad K = \prod_i \nu_i a_i \tag{3}$$

where K is the equilibrium constant corresponding to the reaction of eqn. (1), a_i is the activity of the ith component in the reaction, n is the number of electrons involved in the reaction, F is Faraday's constant, R is the gas constant, T is the absolute temperature.

The general equilibrium reaction, eqn. (1), can be independently categorized depending on the nature of the reactant phase, B. For the case where B is an element, the reaction is a formation reaction and thus ΔG_{rxn} is equivalent to the free energy of formation of the product A_xB. If B is a compound, either of two or more situations may become possible: (i) the formation of a ternary alloy in which the reaction is considered to be insertion and (ii) the disproportionation of the reactant(s) into alloy products of varying compositions and constituents. The second class are generally referred to as reconstitution reactions.

In an insertion reaction (sometimes also refered to as a solid solution reaction), the electroactive species enters, but does not change, the framework structure of the reactant. These reactions are often described as topotactic, and according to the Gibbs phase rule, intrinsic properties such as the chemical potential of the electroactive species, and thus the electric potential of the electrode reactant will vary with composition. The advantage of this type of electrode reaction is that the electrodes are readily reversible since no phase change is involved. However, it has the disadvantage that the electrode potential is composition dependent and there may be a limited compositional range for the electroactive species.

Reconstitution reactions on the other hand involve the formation of new phases. This may lead to a composition-independent value of the electric potential determined by the Gibbs free energies of formation of the phases present. If the number of phases present is equal to the number of components under constant temperature and pressure conditions, Gibbs phase rule specifies that all intensive thermodynamic variables are fixed and independent of the overall composition. Chemical potentials, and thus electrode potentials under equilibrium conditions, are therefore independent of composition. The length of such a constant potential plateau, which represents the ampere-hour capacity of the sample electrode in question, is determined, in the case of a binary system, by the extent of the two-phase equilibrium, and, in the ternary case, by the extent of the three-phase equilibrium. The advantage of a reconstitution reaction is that it can lead to a constant equilibrium potential over a useful compositional range which is essential if high energies are desirable. Such reactions, however, have the disadvantage that their reversibility can be quite slow since the relative amounts of the reactant and product phases change with the extent of reaction.

To understand how these different solid state reactions results from changes in phase equilibria which in turn results from changes in the number of components in a given system, consider a generalized lithium-based binary system, Li–M say, to which appropriate amounts of component N is added, and N forms an alloy, $M_\beta N$, with M. Several examples will be used to illustrate the effects of this addition on the changes in reaction equilibria and thus in either or both of the electrode potential and capacity of Li–M system. In a first example where N does not react with lithium, hypothetically represented in Fig. 1, the reaction of lithium with the metal M to form the alloy

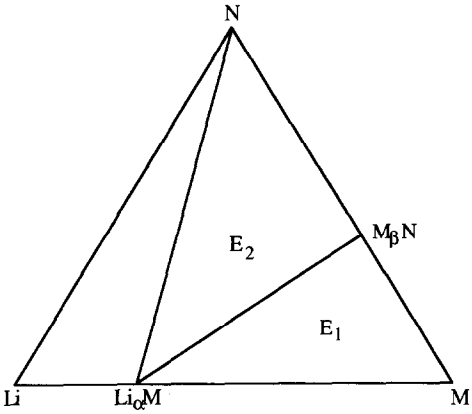

Fig. 1. Schematic representation of a simple Li–M–N ternary system phase diagram for the case where N does not react with lithium.

$Li_\alpha M$ can be represented by the equation

$$M + \alpha Li \rightleftharpoons Li_\alpha M \tag{4}$$

and the reversible potential for this reaction is given by the Nernst relation:

$$E_1 = -\frac{\Delta G_f(Li_\alpha M)}{\alpha F} \tag{5}$$

where α is the number of electrons transfered, and thus, of the number of moles of lithium transferred in reaction (4) and F is Faraday's constant. Small additions of N do not change the voltage of the electrode so long as the overall composition still lies in the triangle labelled E_1. However, on addition of sufficient N that the composition is in the triangle labelled E_2, the voltage of the electrode versus pure lithium changes such that

$$E_2 = -\frac{\Delta G_{rxn}}{\alpha F} < E_1 \tag{6}$$

where ΔG_{rxn} is the Gibbs free energy change of the reaction

$$\frac{1}{\beta} M_\beta N + \alpha Li \rightleftharpoons Li_\alpha M + \frac{1}{\beta} N \tag{7}$$

The consequence of the addition of N is then to make the electrode potential more negative, and thus to increase the voltage of any cell which uses M–N as the negative electrode. The Li/M ratio is still the same as in the triangle labelled E_1, but the weight of the electrode has been increased by the addition of N. Hence, one needs to minimize the amount of N added in order to take advantage of the reduced electrode potential.

An unconcious use of this principle in a practical cell demonstration is the well documented high specific energy sodium/metal chloride ($FeCl_2$ or $NiCl_2$) batteries [11]. In this cell, iron (or nickel) can be treated as the third component in an otherwise binary sodium/chlorine system. By adding appropriate amounts of iron, say, the two component binary reaction

$$Na + Cl \rightleftharpoons NaCl \tag{8a}$$

$$E_1^\circ = -\frac{\Delta G_f(NaCl)}{F} \tag{8b}$$

becomes a three-component reaction represented by the three-phase equilibrium

$$FeCl_2 + 2Na \rightleftharpoons 2NaCl + Fe \tag{9a}$$

$$E_2^\circ = -\frac{\Delta G_r^\circ}{2F} < E_1^\circ \tag{9b}$$

In a second example, illustrated in Fig. 2, where N reacts with lithium, the range of Li/M is increased when one enters the triangle labelled E_3 by the addition of N. The potential of the electrode versus lithium is then given by the reaction

$$\frac{1}{\beta} M_\beta N + \left(\alpha + \frac{\gamma}{\beta}\right) Li \rightleftharpoons Li_\alpha M + \frac{1}{\beta} Li_\gamma N \tag{10}$$

and

$$E_3 = -\frac{\Delta G_{rxn}}{\left(\alpha + \frac{\gamma}{\beta}\right) F} < E_1 \tag{11}$$

Again, the addition of N makes the electrode potential more negative and thus increases the cell voltage. The electrode capacity, expressed in terms of the number of moles of lithium per mole of M, also increases.

In some cases, a multi-phase binary system may not be practically useful over its entire compositional range due to the existence of high voltage plateaus and also poor lithium diffusion in one or more of the phases. A ternary phase diagram such as in Figs. 1 or 2 which involves the binary system in question might therefore increase both the cell voltage and storage capacity of the electrode. The consequence would

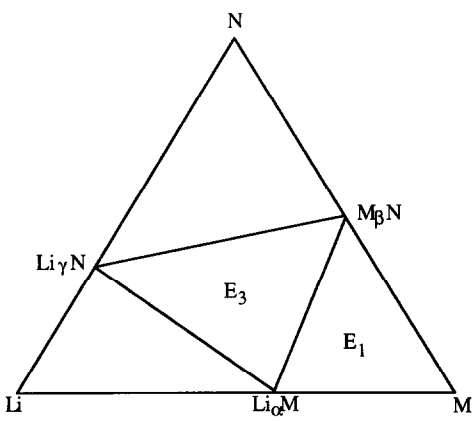

Fig. 2. Schematic of a hypothetical Li–M–N ternary phase diagram for the case where N forms an alloy with lithium.

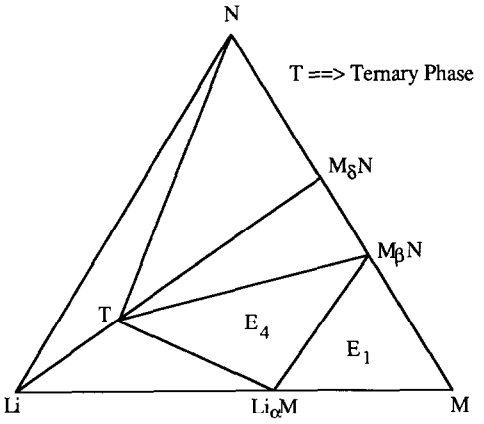

Fig. 3. Schematic representation of a Li–M–N ternary system phase diagram for the case where N does not alloy with lithum, but rather forms a ternary phase, T.

be an increase in the specific energy or energy density if the third component is optimally maximized. In others, the existence of a binary M–N phase may not be necessary if there exists a Li–M–N ternary phase which gives rise to the same geometry in the lower portion of the phase diagram. A hypothetical example is shown in Fig. 3, in which the presence of the ternary phase, T, not only improves the cell voltage ($E_4 < E_1$), but also increases the Li/M ratio. Arguments governing this illustration are the same as in the previous examples.

In general, therefore, a logical starting point for the selection of electrode materials would be a binary system which is well characterized in terms of its potentials and capacities. In seeking the additive component, lightweight materials and those that form high density alloys with M are desirable. In this way, one enhances either the specific energy or energy density as the case may be.

Application to some Li–Si–N systems

Having considered how the addition of a third component to a binary system can alter both the electrode capacity and potential of the binary alloy electrode, let us examine how this changes can occur in a real situation. As an illustration, consider the Li–Si binary system for which thermodynamic properties such as electrochemical potentials and capacities have been well documented. The methodology described above will be applied to some Li–Si-based ternary systems to predict how the addition of a third component to the binary system can result in changes of both intrinsic and extrinsic properties of the system.

A powerful tool for the representation of thermodynamic properties of electrode materials made from solid alloy systems is the equilibrium coulometric titration (electrochemical potential versus composition) curve. This has been carefully measured for the binary Li–Si system at 415 °C [12] and the result is reproduced in Fig. 4. It shows four plateau regions labelled A to D, with potentials 332, 288, 158 and 44 mV positive of pure lithium. Of particular interest here is the plateau marked C, which has a voltage of +158 mV versus lithium and a capacity of about 0.92 mol of lithium per mole of silicon. This theoretical capacity converts to 0.018 mol of lithium per gram total weight, or equivalent, 485 mA h/g. The corresponding maximum theoretical

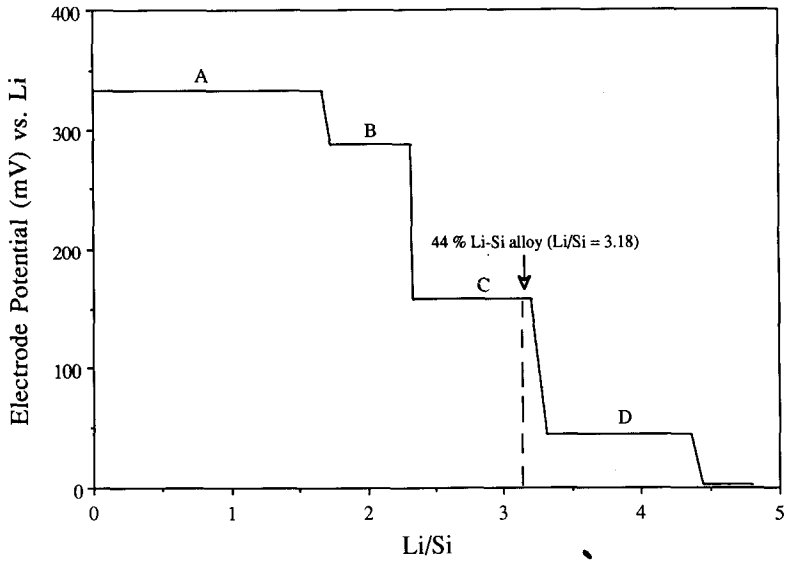

Fig. 4. Equilibrium coulometric titration curve for the Li–Si binary system in a LiCl–KCl eutectic melt at 415 °C (after ref. 12).

specific energy (*MTSE*), when a material on this plateau is used as the negative electrode in a hypothetical cell with a 1 mol Li/60 g active material cathode which is 2.0 V positive of pure lithium, is 428 W h/kg. An electrode from this plateau is thus equivalent to the standard 44 wt.% Li–Si alloy which has an initial value of Li/Si ratio of 3.18, and thus lies near the high-lithium end of the plateau C in Fig. 4. When used as the reactant in the negative electrode of the Li–Si alloy/FeS_2 thermal battery, it acts as the source of lithium, and the overall composition of the electrode component traverses most of plateau C during activation of the battery. Hence, in our consideration, this plateau potential and the corresponding capacity will be used as a baseline against which to compare the potentials and capacities of candidate Li–Si based ternary systems.

Free energies of phases in the Li–Si–N systems

The ternary additions that are considered in this communication include Ca, Cr, Mg, Mn, Mo, Nb, Ni, Ta, Ti and V. For the prediction of the respective Li–Si–N ternary phase diagrams, the relevant thermodynamic information is the Gibbs free energy (or free energy of formation) of all the phases, both binary and ternary, that are known to exist at the appropriate temperature. This information is readily available in the literature [13–16] for most of the phases in these systems. Values for the Li–Si binary system have been calculated from the titration curve of Fig. 4. In some cases where phases have been identified for which there are no free energy values, it is possible to assign approximate free energy values to some of these from information available on their adjacent phases, using the energy minimization/maximization approximation [6]. This analysis, however, has been excluded in this discussion and only free energy values reported in the literature are utilized. Hence, in the interpretation of the thermodynamic reaction equilibria of systems incorporating phases with unavailable energy values, one needs to be extra cautious in treating only the relevant three-phase

tie-triangles. In the Li–Si–Mg system, the $LiMg_2$ phase was excluded from the analysis because of the controversy surrounding its existence. In general, ternary additions have been selected in such a way that the added components do not alloy with lithium, and the melting temperatures of the binary N–Si alloys are greater than 900 °C. This restriction in the choice of materials was necessary in order to screen prospective candidate alloy systems with proper thermodynamic and kinetic properties for use in thermal batteries operating in the 400–450 °C temperature range.

Phase diagrams and potential plateau voltages

Equilibrium isothermal phase diagrams for all the ternary Li–Si–N systems at 400 °C have been constructed from available values of the respective free energies, and assuming point compositions for all the phases. They all show regions of three-phase equilibria, bounded by tie-lines of two-phases equilibria, with three nominal phases at the apexes of each tie-triangle [17]. As mentioned earlier, care must be taken in the interpretation of those systems where energy values are not available for some of the phases. In the phase diagram of the Li–Si–Ni system (Fig. 5) for example, the tie-triangle with Ni, NiSi and $Li_{22}Si_5$ at the apexes cannot be treated as a valid three-phase equilibrium since phases such as Ni_3Si, Ni_5Si_2, Ni_2Si and Ni_3Si_2 have been reported [15, 16] but no thermodynamic data are presently available. All of these phases have compositions that are within the 'Ni–NiSi–$Li_{22}Si_5$' tie-triangle, pointing out an apparent violation of the phase rule, since in a three-component system, it is impossible to have coexistence of more than three phases in equilibrium under isothermal and isobaric conditions.

For any of the given systems, the potential plateau voltage representative of each three-phase equilibrium can be calculated from the appropriate reaction for the tie-triangle in the phase diagram. As an illustration, consider the Li–Si–Mo system in which the phase diagram at 400 °C is shown in Fig. 6. The addition of molybdenum to the binary Li–Si system gives rise to two additional equilibria not originally present in the binary system. These are identified by I and II in the diagram. The reconstitution reactions corresponding to these equilibrium tie-triangles are respectively

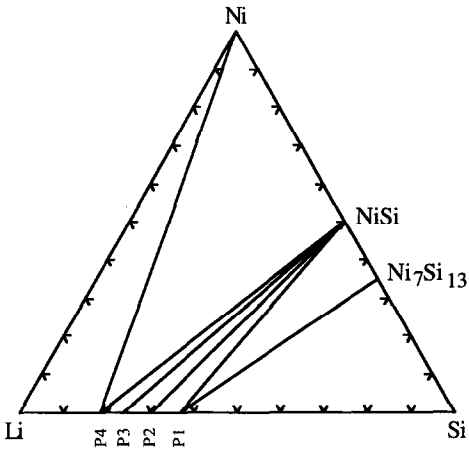

Fig. 5. Estimated Li–Si–Ni ternary phase diagram at 400 °C, P1, P2, P3 and P4 are the $Li_{12}Si_7$, Li_7Si_3, $Li_{13}Si_4$ and $Li_{22}Si_5$ phases in the Li–Si binary system.

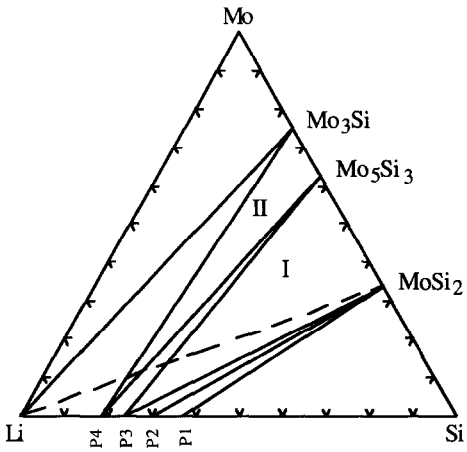

Fig. 6. Illustrative phase diagram for the Li–Si–Mo ternary system at 400 °C. The phases P1, P2, P3 and P4 are the same as in Fig. 5. I and II represent regions of the three phase equilibria $MoSi_2$–Mo_5Si_3–$Li_{13}Si_4$ and Mo_5Si_3–Mo_3Si–$Li_{22}Si_5$, respectively.

$$20MoSi_2 + 91Li \rightleftharpoons 4Mo_5Si_3 + 7Li_{13}Si_4 \quad (12)$$

and

$$15Mo_5Si_3 + 88Li \rightleftharpoons 25Mo_3Si + 4Li_{22}Si_5 \quad (13)$$

The Gibbs free energy change for these reactions are −251.712 and −5.48 kcal, respectively. The corresponding thermodynamic reversible potentials estimated from the Nernst relation $E = -\Delta G_{rxn}/nF$ are +120 and +3 mV versus pure elemental lithium. Hence, if a hypothetical electrode is made from an alloy of composition $MoSi_2$, say, then under discharge conditions, i.e. on addition of lithium to the electrode, the composition of the electrode, and thus the lithium activity as well as the electrode potential, will move from $MoSi_2$ towards lithium, crossing regions of both three-phase and two-phase equilibria, following the path indicated by the dashed line in the phase diagram. The useful portion in this system is that within the tie-triangle marked I for which the extent of reaction along the dashed line is 24.8 mol of Li per kilogram total electrode weight corresponding to an overall capacity of 664 mA h/g.

Estimated thermodynamic electrode potentials corresponding to the other three-phase equilibria in these Li–Si–N systems are reported in Table 1 as voltages positive of pure lithium.

Electrode capacities and specific energies

In addition to electrode potentials, the lithium capacities for all the three-phase equilibria in the systems listed above have been estimated both in terms of moles of lithium per mole of silicon involved in the reaction and as moles of lithium per gram total weight. The latter values are easily converted to the usual dimensions of A h/g with a multiplication factor of 26.8. The estimated maximum theoretical values for the various equilibria are shown in Table 1. Materials that would make better negative electrodes are those with both relatively negative electrode potentials corresponding to high cell voltages, and those with high lithium capacities. From a practical point of view, however, materials with electrode potentials very close to pure lithium

TABLE 1

Estimated thermodynamic properties of several Li–Si-based ternary systems

System[a]	Starting composition	Phases in equilibrium	Electrode potential (mV vs. Li)	Electrode capacity		*MTSE* (W h/kg)
				Li/Si	Li/g ($\times 10^3$)	
Li–Si	Li_7Si_3	Li_7Si_3–$Li_{13}Si_4$	158	0.92	18.1	428
A–Mg	Mg_2Si	Mg_2Si–Mg–$Li_{13}Si_4$	60	3.25	32.7	574
A–Mn	MnSi	MnSi–Mn_5Si_3–Li_7Si_3	163	0.93	10.4	316
	Mn_5Si_3	Mn_5Si_3–Mn_3Si–$Li_{13}Si_4$	45	1.44	11.1	350
	Mn_3Si	Mn_3Si–Mn–$Li_{33}Si_5$	43	4.40	19.7	474
A–Mo	$MoSi_2$	$MoSi_2$–Mo_5Si_3–$Li_{13}Si_4$	120	2.28	24.8	502
	Mo_5Si_3	Mo_5Si_3–Mo_3Si–$Li_{22}Si_5$	3	1.96	9.7	328
A–Ni	Ni_7Si_{13}	Ni_7Si_{13}–NiSi–$Li_{12}Si_7$	316	0.79	12.1	317
A–Nb	$NbSi_2$	$NbSi_2$–Nb_5Si_3–Li_7Si_3	184	1.63	19.0	432
A–Ta	$TaSi_2$	$TaSi_2$–Ta_5Si_3–Li_7Si_3	211	1.63	12.6	344
A–V	VSi_2	VSi_2–V_5Si_3–Li_7Si_3	191	1.63	25.2	486
A–Ca	CaSi	CaSi–Ca_2Si–$Li_{22}Si_5$	13	2.2	26.4	544
A–Cr	$CrSi_2$	$CrSi_2$–CrSi–Li_7Si_3	223	1.17	18.8	420
	CrSi	CrSi–Cr_5Si_3–Li_7Si_3	205	0.93	10.8	315
	Cr_5Si_3	Cr_5Si_3–Cr_3Si–$Li_{13}Si_4$	138	1.44	11.6	341
A–Ti	TiSi	TiSi–Ti_5Si_3–Li_7Si_3	182	1.55	11.3	328

[a]A = Li–Si.

may not necessarily be attractive after all, since the lithium activity in these materials can be exceedingly high. This high value of lithium activity will often lead to high reactivity in dry air, and thus difficulties in handling.

Also included in Table 1 are the values of maximum theoretical specific energy (*MTSE*) in units of W h/kg for the respective ternary reaction plateaus. These *MTSE* values were obtained by using the expression:

$$MTSE = \frac{26.805 n E_{av}}{W} \tag{14}$$

where n is the number of moles of lithium transferred during the cell reaction, E_{av} is the difference between the positive and negative electrode potentials in volts, and W is the total weight of active electrode materials only, expressed in kilograms. For these estimates, a material with a capacity of one lithium in every 60 g of active component and a potential of +2.0 V versus pure elemental lithium was used as the reference positive electrode.

Discussion and conclusions

Based on these thermodynamic estimates, three systems, Li–Si–Ca, Li–Si–Mg and Li–Si–Mo appear to show promise as prospective negative electrodes with properties that could lead to improved battery characteristics when used in intermediate temperature

thermal cells. Estimated thermodynamic properties for these three systems have been isolated and are compared with the corresponding values for the Li–Si binary system in Table 2.

For the Li–Si–Mo ternary alloy system, a starting composition corresponding to $MoSi_2$ will yield an electrode with a potential increment of about 40 mV over the conventional Li–Si binary alloy. This value corresponds to a loss of 120 mV when compared with elemental lithium (cf. losses of 300 and 160 mV for the Li–Al and Li–Si systems, respectively). Even more staggering are the potentials for the Li–Si–Mg and Li–Si–Ca systems utilizing the three-phase equilibria Mg_2Si–Mg–$Li_{13}Si_{14}$ and CaSi–Ca_2Si–$Li_{22}Si_5$, respectively. These values convert to theoretical increments of 98 and 145 mV, respectively, over the binary Li–Si system. Potential losses with respect to elemental lithium are only 60 and 13 mV, respectively, for these systems. However, and as explained earlier, the low electrode potential and thus high lithium activity of the Li–Si–Ca system may lead to high reactivity and containment problems of the Ca-based alloy when used in a practical cell.

The lithium storage capacities of the ternary Ca-, Mg- and Mo-based alloys have also been increased relative to the 44 wt.% Li–Si binary system. The equivalent capacity values in units of mA h/g are 707, 876 and 665, respectively, which are to be compared with 485 for the binary system. These numbers correspond to increments of 46, 80 and 37%, respectively.

Considering only active electrode materials with the hypothetical reference cathode described in the text, the maximum theoretical specific energies (W h/kg) of these three systems are Ca, 544; Mg, 574; Mo, 502. These values, compared with 428 W h/kg for the Li–Si binary system represent increases of 27, 34 and 17%, respectively. These percentage increments in the energy values will even be higher when compared on a volumetric basis because of the higher density of the ternary alloys. The analysis and discussions above clearly suggest that ternary, or even more

TABLE 2

Comparison of the thermodynamic properties of candidate ternary electrode materials with those of the binary Li–Si system

System	Electrode potential (mV vs. Li)	Electrode capacity		Specific energy of cell[a] (W h/kg)
		Li/Si	Li/kg	
Li–Si				
Li_7Si_3–$Li_{13}Si_4$	158	0.92	18.1	428
Li–Si–Mg				
Mg_2Si–Mg–$Li_{13}Si_4$	60	3.25	32.7	574
Li–Si–Mo				
$MoSi_2$–Mo_5Si_3–$Li_{13}Si_4$	120	2.28	24.8	502
Li–Si–Ca				
CaSi–Ca_2Si–$Li_{22}Si_5$	13	2.20	26.4	544

[a]specific energy $= \frac{\int_{\text{capacity}} (\text{cell voltage})}{\text{weight}}$ where cell voltage = potential difference between alloy electrode and hypothetical positive electrode defined in text.

so, quaternary modifications of binary alloy systems could lead to materials with better battery electrode characteristics. The question of how these materials will perform when tested in a practical cell, or half-cell for that matter, remains to be answered, and forms the basis of the second part of these series of publications [18, 19]. The results of experiments conducted with the Li–Si–Mg system are reported and discussed in these publications.

Acknowledgement

Financial support for this work has been provided by Sandia National Laboratory under contract No. 53-3321.

References

1 N. P. Yao, L. A. Heredy and R. C. Saunders, *J. Electrochem. Soc., 118* (1971) 1039.
2 E. C. Gay, D. R. Visers, F. J. Martino and K. E. Anderson, *J. Electrochem. Soc., 123* (1976) 1591.
3 R. N. Seefurth and R. A. Sharma, *J. Electrochem. Soc., 124* (1977) 1207.
4 R. N. Seefurth and R. A. Sharma, *J. Electrochem. Soc., 127* (1980) 1101.
5 B. E. Liebert, *Ph.D. Dissertation,* Stanford University, 1977.
6 N. A. Godshall, *Ph.D. Dissertation,* Stanford University, 1980.
7 C. Li-Chuan and W. Weppner, *Naturwissenschaften, 65* (1978) 595.
8 W. Weppner, C. Li-Chuan and W. Piekarczyk, *Z. Naturforsch., Teil A, 35* (1980) 381.
9 W. Weppner, C. Li-Chuan and A. Rabenau, *J. Solid State Chem., 31* (1980) 257.
10 N. A. Godshall, in J. B. Boyce, L. C. DeJonghe and R. A. Huggins (eds.), *Proc. 5th Int. Conf. Solid State Ionics,* Vols. 18 and 19, Elsevier, Amsterdam/New York, 1986, p. 788.
11 R. C. Galloway, *J. Electrochem. Soc., 134* (1987) 256, and refs. therein.
12 C. J. Wen and R. A. Huggins, *J. Solid State Chem., 37* (1981) 271.
13 M. Hansen and K. Anderko, *Constitution of Binary Alloys Series,* McGraw-Hill, New York, 1958.
14 J. B. Clark, (ed.), *Bulletin of Alloy Phase Diagram,* ASM International.
15 I. Barin, O. Knacke and O. Kubaschewski, *Thermochemical Properties of Inorganic Substances,* Springer, Berlin, 1973 and 1977.
16 P. Nash and A. Nash, *Bull. Alloy Phase Diagram, 8* (1987) 6.
17 *Annual Progress Rep.,* Contract Sandia 53-3321, Sandia National Laboratory, Albuquerque, NM, Oct. 1987.
18 A. Anani and R. A. Huggins, *J. Power Sources, 38* (1992) 1374.
19 R. A. Huggins and A. Anani, *US Patent 4 950 556* (1990).